



Optimization and neural modelling of infiltration rate in ultrasonic machining

Ravinder Kataria¹ · Ravi Pratap Singh²  · M. H. Alkawaz³ · Kanishka Jha¹

Accepted: 3 May 2021 / Published online: 8 May 2021
© Operational Research Society of India 2021

Abstract

Ultrasonic machining is a processing method typically practiced for processing the highly brittle/hard materials. The proposed research work is attempted at exploring the influence of varying input conditions namely; cobalt %, power rating, thickness of work, different tools, tool geometry, and abrasive size on the infiltration rate in ultrasonic drilling of WC–Co composite through neural modelling. The design of experiments methodology has been practiced for scheming out the experiments. The significant process variables have been acknowledged using variance analysis test which has revealed the abrasive size, power rating, and tool profile as the most influential factors for the infiltration rate. An artificial neural network (ANN) model is suggested to analyze the infiltration rate in USM with striking parameters. Multiple layer feed forward neural architecture is restrained through error-back propagation-based training algorithm. Predicted results show the effectiveness of the proposed neural structure with maximum error of 6%. The optimized parametric combination for infiltration rate has been revealed as; cobalt- 6%, work thickness- 3 mm, tool- hollow, tool material- nimonic-80A alloy, abrasive size- 200, and power rating- 80%. Microstructure analysis revealed that good edge quality with no appearance of cracks or burr/chipping on the edge of the drilled holes which further ensured the quality level of hole drilling through attempted work.

Keywords ANN · Infiltration rate · Neural Modelling · Optimization · Taguchi · USM · WC–Co composite

✉ Ravi Pratap Singh
singhrp@nitj.ac.in

¹ School of Mechanical Engineering, LPU, Jalandhar, Punjab, India

² Department of IPE, Dr. B. R. Ambedkar National Institute of Technology, Jalandhar, Punjab, India

³ Faculty of Manufacturing Engineering, Universiti Teknikal Malaysia Melaka, Melaka, Malaysia

1 Introduction

Ultrasonic machining (USM) is an unorthodox machining solution typically employed for processing brittle/hard materials such as; ceramics, quartz etc. [1, 2]. Singh and Singhal [1] optimized the machining characteristics in ultrasonic assisted rotary machining of alumina ceramic material. It was reported that; feed rate is the most significant factor which affect the machining performances vitally. Cheema et al. [3] optimized the process parameters for wear ration, hole over size and roughness. Results show that abrasive size and power % are major momentous inputs.

Patra [4] discussed the effect of micro-rods invented to drill micro-holes in USM method, results revealed that higher rubbing actions leads to the conclusion that side walls of micro-holes are subjected to early originated cracks. Kataria et al. [5] reported that optimized setting of input parameters, showed an enhancement of 20% in the Grey relation fuzzy grade has been observed, as compared to initial setting. Singh and Singhal [6–8] reported the optimized results in rotary type ultrasonic machining of different ceramic materials. Wang et al. [9] reported the hardening of work on the surface of austenitic steel tool whereas the internal portion was remained flexible and ensures slow tool wear. Singh et al. [10] scrutinized the hole quality measures while attempting the ultrasonic assisted rotary machining of silicon based ceramic. Jadoun et al. [11] reported the drilled hole accuracy in the USM of a ceramic material (alumina). From the results it is found that the size of abrasive grit was the most significant factor in deciding the hole quality. In another investigated, the effect of power rating, grit size, thickness of work, tool material, composition of work material and profile of tool for the TWR and MRR in USM of WC–Co. Results concluded that the main leading parameter was grit size [12].

WC–Co usually consists of grains of tungsten carbide inserted in a metal-binder phase, which reflects high hardness to resist attrition and adequate toughness to stand against interrupted incisions or vibration generated during the machining [13]. Hot abrasive jet machining (HAJM) has been suggested to attempted for various operations such as drilling, surface etching, grooving and micro finishing on the glass and ceramics [14]. The commercially available composition of cobalt–tungsten carbide can vary greatly; its composition normally ranges from 50 to 97% WC (with the presence of other metallic carbides such as tantalum carbide or titanium carbide) and from 3 to 16% cobalt. Most common and commercially acclaimed manufacturing route for the Cobalt-Bounded-Tungsten carbides hard materials is through Powder Metallurgy, which is consisting of Tungsten carbide powder generation, its consolidation, liquid phase sintering and post-sintering sequences. Hard materials like WC–Co composites have better mechanical properties, by the virtue of these properties, they possess many industrial solicitations i.e. production of punch, wear parts, die, drilling and cutting tools.

Based on the above elaborate issues and gaps observed, the present research work has been targeted to study the infiltration rate, which has very rarely

been attempted in past researches while processing the tungsten carbide–cobalt (WC–Co) composite with ultrasonic machining (USM) method. The infiltration rate is the term which describes about the rate of indentation or penetration (cutting capacity per unit of length undertaken) during the ultrasonic machining of considered composite material. For evaluating the machining capability of any process, it is needed to explore its overall machining performance in terms of different machining characteristics. The utility of artificial neural network-based modeling and optimization is another novel attempt made for the present research investigation. The consideration of some specific input variables i.e. tool profile, work thickness, etc. further makes the work more interesting in the current scenario of advanced processing of composites.

The basic principle and working mechanisms of USM process has been discussed in introduction section. The details about the set-up used and material selection have been explored in second section of the paper i.e. materials and methods. The third section on results and discussion is detailing about the findings (machining output) after applying the design of experiments in terms of taguchi's approach and novel artificial neural network method to optimize the process parameters for achieving optimum level of infiltration rate in USM of WC–Co composite material. The conclusion section is provided to report the major research findings in more precise manner.

2 Materials and methods

This article investigates the effect of different process parameters on infiltration rate in USM of WC–Co material composite. For the identification of various influential variables for infiltration rate in ultrasonic drilling operation, fish-bone diagram (Fig. 1) was designed. In present research, materials to be worked on were selected with 6% and 24% cobalt content and thickness of 3 mm and 5 mm were used. Tool

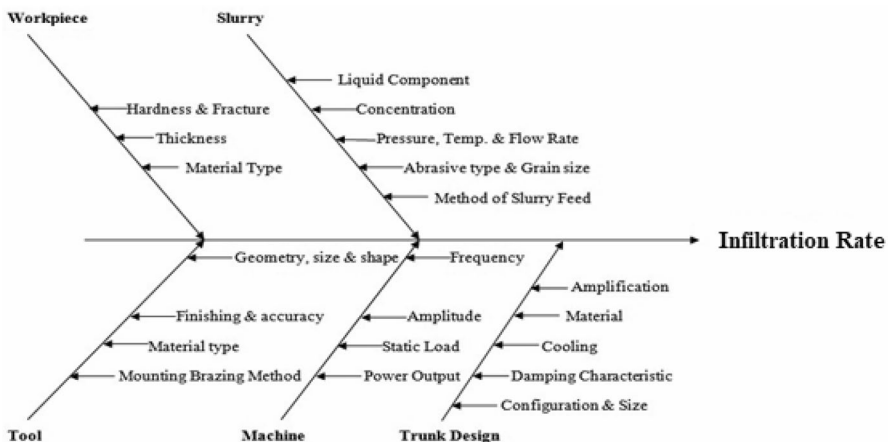


Fig. 1 Cause and effect diagram

Table 1 USM Process Parameters and Levels

Emblem	Inputs	Level 1	Level 2	Level 3
A	Cobalt (wt%)	6%	24%	-
B	Work Thickness	3 mm	5 mm	-
C	Tool Profile	Solid	Hollow	-
D	Tool material	Stainless steel	Silver steel	Nimonic-80A
E	Grit size (μm)	74	44	25
F	Power rating	40%	60%	80%

was provided with two different geometries namely; solid and hollow. Abrasive used in the study was Boron carbide. Table 1 explores the various levels of inputs for employing DOE. The selection of parameters and their levels for main experiments has been made based on the conducted pilot or trial runs [4, 5]. These trial runs have been performed based on one-factor at a time approach i.e. varying one factor/parameter at a time (tool, work material, grit size, power rating, and abrasive) and keep the remaining factors at some fixed values (tool: stainless steel; grit size: 200 mesh; abrasive: boron carbide; power rating: 40%). The effects of these trial runs have been observed by looking into their influences over the considered process characteristics for trial runs. Therefore, the final values of input parameter levels decided accordingly where the factors were influencing the considered responses more impressively [6, 12].

The setup used for performing all set of experiments was an ‘AP-450 model’ USM. Figure 2 clearly shows the arrangement of various constituents of USM setup namely; Slurry pump, coupler, transducer, slurry tank, etc. Machining region primarily contains work-piece and fixture on mill stand, and tool, all are represented in Fig. 2. For recording experimental time for each run a stop watch was attached. Infiltration rate was calculated as a fraction of depth of hole (drilled) to time for operation, for a quantified depth. For the pilot experimentation, blind holes upto the depth of 1 mm were drilled in workpiece, as shown in Fig. 3. Tools were designed in a such a way that, each one is having equal weight. The mass of each tool was fixed to 9 g, in order to ensure the vibration of the tools at the resonant frequency, as per the specification of the manufacturer (Sonic-Mill, USA). The mass of tool become further more crucial when it comes to machine with hollow tool with very fine dimensions. All the tools were fabricated as single piece unit by turning using a centre lathe machine. The detailed geometries of tool all well illustrated in Fig. 4.

Taguchi’s theory based orthogonal matrix (L_{36}) was selected for experimental plan, because plan is consisted of mixed level factors and also to study the interaction between the factors. Overall 6 factors were analyzed for experiment and with variation in levels which made them mixed in nature, same was explained by Taguchi and many researchers also used the design for designing the experiments [13, 15]. By selecting L-36 design, the minimum requirement for degree of freedom was fulfilled as required was 15(DOF) and available with L-36 was 35(DOF). The strategic experiments are displayed in Table 2. Two replicate runs were also incorporated

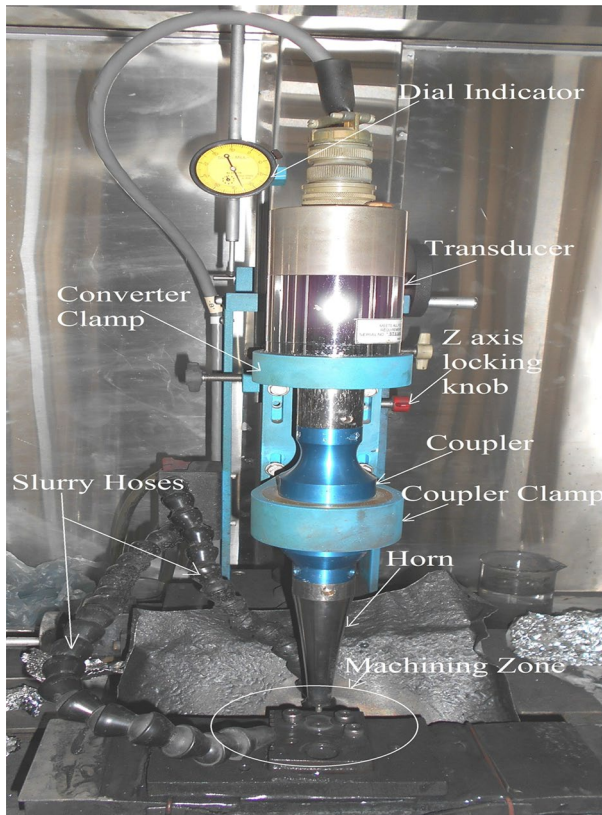


Fig. 2 USM set-up used for experimentation

in the schemed tests with all runs in randomize order, to curtail all nuisance present in the experimental plan.

Larger the best

$$\left(\frac{S}{N}\right)_{LB} = -10\text{Log}\left(\frac{1}{R} \sum_{j=1}^R \frac{1}{y_j^2}\right) \quad (1)$$

3 Results and discussion

After analyzing the outcomes conquered with variance test, the influence of each input factor on infiltration rate has been studied. In this section variation drifts for several responses have been perceived and discussed. Figure 5 illustrates the normal probability plots of residuals for infiltration rate. It was discovered that the residuals



Fig. 3 Holes drilled in workpiece during pilot experiments

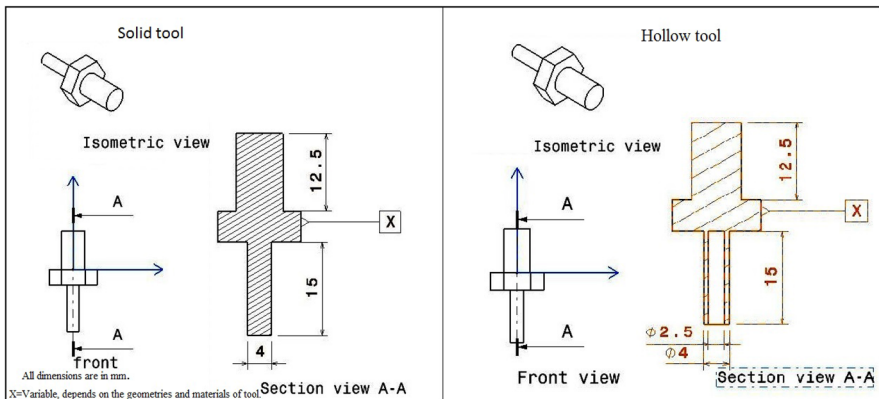


Fig. 4 Detailed drawings of tools used

were dwindling on straight contour, which implies inaccuracies are normally spread-out. This validates the model conventions made for variance test (ANOVA).

As per the mean effect plot (Fig. 6) for infiltration rate, Cobalt wt% has no substantial effect on the infiltration rate within defined levels. Plot also shows the effect of work piece thickness on infiltration rate in a manner that if work piece thickness increases it resulted in a consistent decrement in IR, because feeding of slurry to the work zone hampers drastically which also affect the MRR. The similar behaviors have also been reported by past investigators in the same domain [2–4]. Study also reveals that the Tool’s Profile also have noteworthy effect on the infiltration rate, hollow tool gives enhanced abrasive flow than solid tool which is the dominant

Table 2 Experimental plan with Response

Exp No	Inputs						IR ($\mu\text{m}/\text{sec.}$)			
	A	B	C	D	E	F	IR 1	IR 2	Mean	S/N ratio
1	1	1	1	1	1	1	1.077	0.928	1.003	-0.049
2	1	1	1	1	2	2	1.060	1.183	1.122	0.957
3	1	1	1	1	3	3	1.282	0.933	1.108	0.563
4	1	2	2	1	1	1	0.632	0.398	0.515	-6.438
5	1	2	2	1	2	2	1.308	1.600	1.454	3.121
6	1	2	2	1	3	3	1.335	1.118	1.227	1.672
7	2	1	2	1	1	1	0.957	0.515	0.736	-3.858
8	2	1	2	1	2	2	1.398	2.098	1.748	4.326
9	2	1	2	1	3	3	1.512	1.360	1.436	3.105
10	2	2	1	1	1	1	0.493	0.632	0.563	-5.195
11	2	2	1	1	2	2	0.678	0.783	0.731	-2.790
12	2	2	1	1	3	3	0.885	0.583	0.734	-3.238
13	1	1	1	2	1	2	1.628	1.422	1.525	3.605
14	1	1	1	2	2	3	1.958	2.458	2.208	6.713
15	1	1	1	2	3	1	0.197	0.383	0.290	-12.129
16	1	2	2	2	1	2	1.798	1.935	1.867	5.403
17	1	2	2	2	2	3	3.437	3.762	3.599	11.097
18	1	2	2	2	3	1	0.373	0.453	0.413	-7.796
19	2	1	2	2	1	2	2.087	2.012	2.049	6.227
20	2	1	2	2	2	3	2.962	3.115	3.038	9.644
21	2	1	2	2	3	1	0.247	0.395	0.321	-10.577
22	2	2	1	2	1	2	0.843	1.070	0.957	-0.568
23	2	2	1	2	2	3	1.398	1.325	1.362	2.672
24	2	2	1	2	3	1	0.205	0.347	0.276	-12.057
25	1	1	1	3	1	3	3.427	4.098	3.763	11.405
26	1	1	1	3	2	1	1.103	0.873	0.988	-0.278
27	1	1	1	3	3	2	0.533	0.463	0.498	-6.113
28	1	2	2	3	1	3	3.258	3.795	3.527	10.871
29	1	2	2	3	2	1	0.712	0.540	0.626	-4.316
30	1	2	2	3	3	2	1.647	1.445	1.546	3.727
31	2	1	2	3	1	3	4.153	4.815	4.484	12.962
32	2	1	2	3	2	1	1.367	0.955	1.161	0.883
33	2	1	2	3	3	2	0.812	0.627	0.719	-3.079
34	2	2	1	3	1	3	2.735	2.913	2.824	9.004
35	2	2	1	3	2	1	0.658	0.715	0.687	-3.287
36	2	2	1	3	3	2	0.370	0.457	0.413	-7.817

parameter to affect the infiltration rate. Hollow tools possess better inertia, effective distribution of abrasive particles during the machining, and less surface area. These traits contribute in the increasing of IR. Different tool material has different effect on IR, nimonic-80A produces maximum IR in the workpiece whereas stainless and

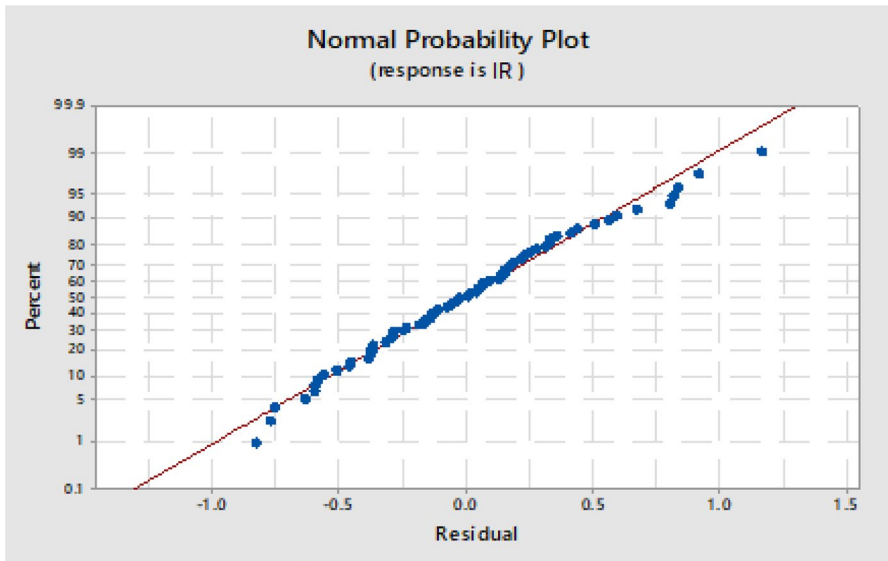


Fig. 5 Normal Probability plot for infiltration rate

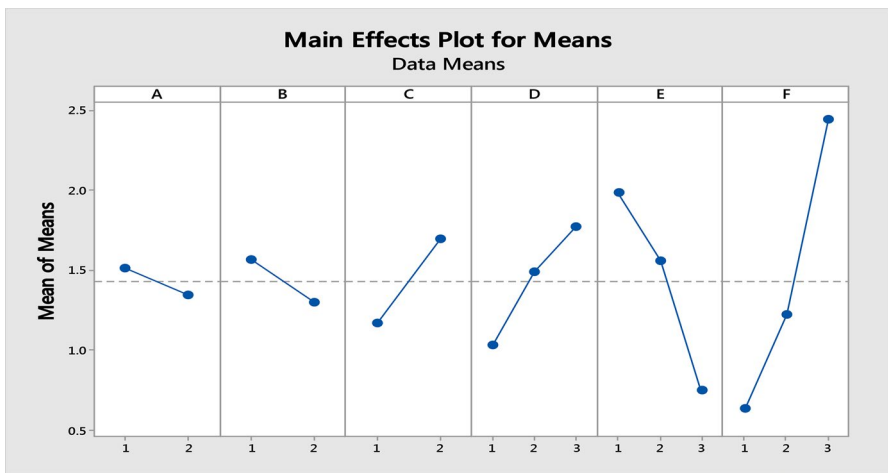


Fig. 6 Mean effect plots for infiltration rate (raw data)

silver steel have contributed less towards IR. This basically depends on the whether both the tool and workpiece are shows higher hardness values. The result shows that nimonic-80A tool (with superior hardness values) contributes the deeper dents into the work surface, stimulating the increased rate of machining.

Two more factors which influence the IR in the work material are abrasive grain size and power rating. Grit size is directly proportional to IR, increase in grit size signifies increase in weight and hence contribute to higher impact force

which results in greater dimension of micro-chips removal from the work material as well from tool contact surface. Such behaviors have also been revealed by past researchers in the similar domain [3, 12]. Power rating relates with energy by which the abrasives are colliding the work surface, therefore if power rating is increased, it further augments the energy of the abrasive particles, thus increasing IR.

For production point of view, infiltration rate must be higher to meet present industry scenario. So, as a response it must be treated as “larger the best”, therefore higher IR is desirable. Infiltration rate is “larger the best” type outcome. So, the desired value is high for IR. As reflected in Fig. 6, the finest input setting for infiltration rate is; cobalt- 6%, thickness of work- 3 mm, material for tool- nimonic-80A alloy, tool profile- hollow, size of abrasive- 200 (mesh), and power- 80%. The main consequence graph for S/N ratio is presented in Fig. 7. The S/N ratio is attained to be premier at these settings, which signals the intensification of the preferred outcome value with least influence of noise. The relative influences for raw data and S/N data have been exposed in Figs. 8, 9. There are no any significant interactions between the factors.

To appraise the connotation of the considered inputs that contribute to the deviation in infiltration rate, the variance analysis test was executed. The raw data of ANOVA test for infiltration rate are shown in Table 3. Grit size, tool material, power rating and tool profile are the most significant parameters for raw data. Additionally, no interactive relationship is significant, as explored in Table 3. Based on raw data variance analysis test results for infiltration rate, the input factors could be arranged in descendent order of their importance as; power (47%), abrasive size (22%), tool material (7.7%), tool profile (5.72%), work thickness (1.52%), and cobalt % (0.58%). Table 4 also illustrates the variance test results for the infiltration rate (S/N data).

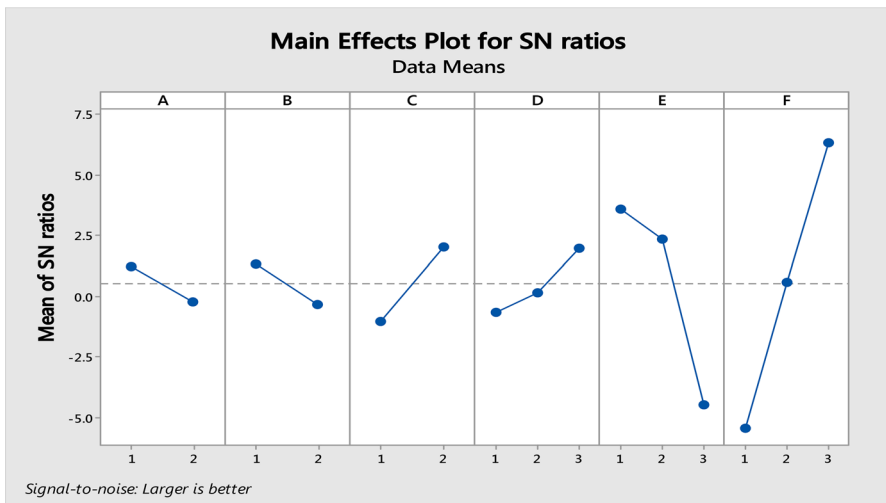


Fig. 7 Mean effect plots for infiltration rate (S/N data)

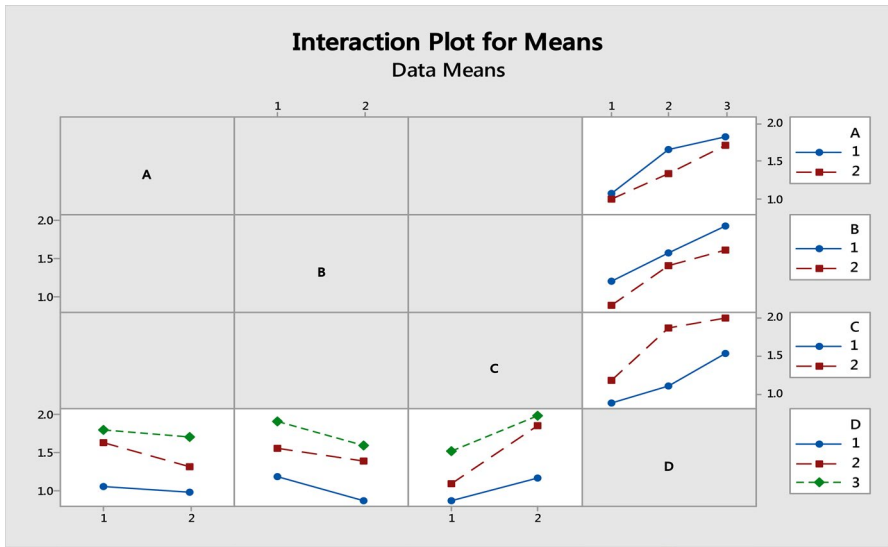


Fig. 8 Interaction plot for Interaction plots (raw data)

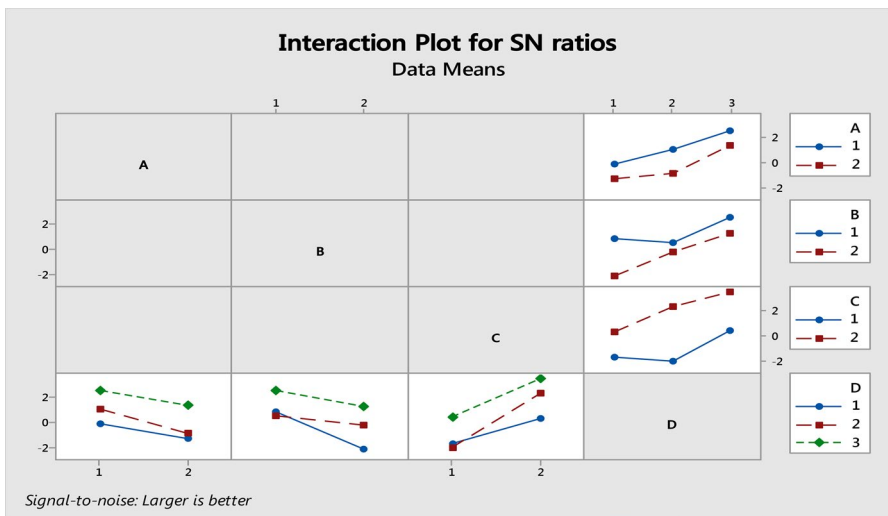


Fig. 9 Interaction plot for Interaction plots (S/N data)

Figure 10 shows the edge quality of hole drilled in WC-6%Co (for Exp. no. 30) at the magnification of 100× and 200×. It can be concluded that the edge quality is good and there is no appearance of cracks or burr/chipping on the edge. The entrance side of the hole depicts a smooth surface.

Table 3 ANOVA outcomes for IR (Raw data)

Source	DOF	Seq SS	Adj SS	Adj MS	F	P
A	1	0.001846	0.001846	0.001846	2.46	0.122
B	1	0.004755	0.004755	0.004755	6.34	0.015*
C	1	0.017727	0.017727	0.017727	23.63	0.000*
D	2	0.024052	0.024052	0.012026	16.03	0.000*
E	2	0.068141	0.068141	0.034071	45.42	0.000*
F	2	0.147472	0.147472	0.073736	98.30	0.000*
A×D	2	0.000717	0.000717	0.000359	0.48	0.622
B×D	2	0.000402	0.000402	0.000201	0.27	0.766
C×D	2	0.002432	0.002432	0.001216	1.62	0.207
Error	56	0.042007	0.042007	0.000750		
Total	71	0.309553				

A-cobalt content, B-thickness of work piece, C- profile of tool, D-material of tool, E-grit size, F-power rating

*Significant at 95% confidence level

S=0.0273886 R-Sq= 86.43% R-Sq(adj)= 82.79%

Table 4 ANOVA outcomes for IR (S/N data)

Source	DOF	Seq SS	Adj SS	Adj MS	F	P
A	1	18.216	18.216	18.216	3.15	0.091
B	1	25.293	25.293	25.293	4.37	0.050*
C	1	85.805	85.805	85.805	14.83	0.001*
D	2	44.040	44.040	22.020	3.81	0.040*
E	2	456.711	456.711	228.355	39.47	0.000*
F	2	835.248	835.248	417.624	72.18	0.000*
A×D	2	1.140	1.140	0.570	0.10	0.907
B×D	2	8.027	8.027	4.014	0.69	0.511
C×D	2	8.306	8.306	4.153	0.72	0.500
Error	20	115.712	115.712	5.786		
Total	35	1598.497				

A, cobalt content; B, thickness of work piece; C, tool profile; D, tool material; E, grit size; F, power rating

*Significant at 95% confidence level

S=2.40532 R-Sq=92.76% R-Sq(adj)=87.33%

3.1 ANN model

The most complex and exciting product of evolution is human brain. Till date it is also the most powerful data processing tool available. On the other hand, Artificial Neural Network (ANN) is a systematic system whose architectural theme is extracted from Biological Neural Networks (BNN) [16]. Human brain learns from examples and parallel processing with the help of neural network which is linked with numerous neurons. ANN model is highly motivated by the human brain that

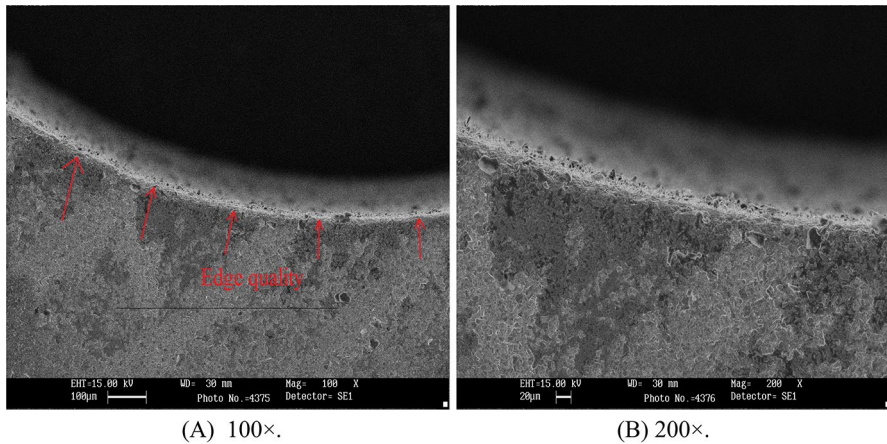


Fig. 10 Edge quality of USMed hole

can train with the help of a teacher, who specifically defines the right responses to input variables [17]. Both ANN and BNN are similar in many ways, to summarize similarities a comparison chart is presented in Table 5 and presented in Fig. 11 [18].

As in ultrasonic machining mathematical equations don't predict actual values because this process is very random in nature and all responses are highly correlated. Hence data is employed to model such speculative methods by ANN tactic grounded on error back-propagation. Using neural network gives an advantage to easily design a model founded on provided input, whereas outcome is proficient, according to input data, to forecast method robustness. ANN approach is recommended in various methods where a sufficient knowledge of the realistic mechanism is quite tough to grasp similar like in the content of ultrasonic machining.

3.2 Prediction of infiltration rate

A neural network consists of a minimum of two physical constituents, called dispensation elements and the interconnection amid them. The dispensation elements in a neural environment known as neurons and the interconnection between these neurons are called as linkages [19]. Each linkage has a unique influence (weight) factor concomitant with it. Individual neuron accepts provocation input from adjacent neurons which are connected to it by linkages, they further process the information and contributes in the form of output. There are several conducts through which the intimation can be treated by a neuron and various means of concerning the neurons to another one. Several neural mesh arrangements can be built by employing distinct dispensation elements and through precise means in which they are associated.

Ultrasonic machining was modeled by multi-layer feed forward neural architecture, which contains of three main layers: input, hidden, and output layers. The input layer is consisting of 6 neurons which signify the six input parameters and one neuron in output layer. The node transition functions are the logsig and tansig functions [19], shown by following Eqs.

Table 5 Similarity between BNN and ANN

Criteria	BNN	ANN
Processing	Slow, parallel but better than ANN	Fast, parallel but not better than BNN
Size	10^{11} neurons	10^2 to 10^4 nodes (depends on application and designer)
Learning	Tolerate ambiguity	Precise and structured data is required to tolerate ambiguity
Fault tolerance	Partial damage degrades the performance	Robust performance
Storage capacity	Storage in Synapse	Storage in continuous memory locations

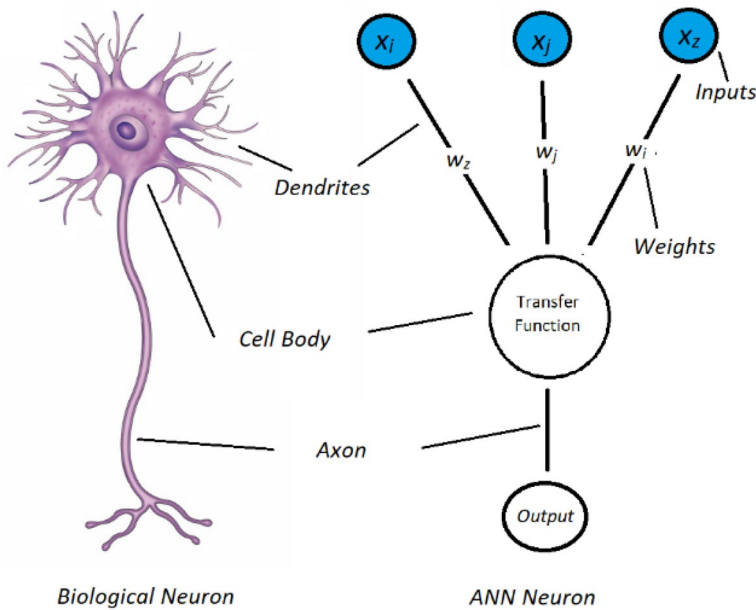


Fig. 11 Structural similarity between BNN and ANN

$$f(x) = \frac{1}{1 + e^{-2x}} \tag{2}$$

$$f(x) = \frac{1}{1 + e^{-2x}} - 1 \tag{3}$$

The neural network structure shown in Fig. 12 contains 6 input neurons and 10 neurons in hidden layer. Network was trained with data set of 16 experiments and validation was performed for 9 experiments. The sum-squared error was minimized with high iteration numbers of 10,000 iterations (Table 6). Further increasing the iterations gives constant output, or in other words no more error. The learning data of ANN for Infiltration rate was shown in Fig. 13. As mentioned earlier, the ANN trained model was validated for accuracy using the experimental values selected from the experimental result which had not been used for the training the network. The comparative representation of the forecasted and investigated values of infiltration rate for the authentication of data set is reflected in Fig. 14. It has been revealed from the plotted results that the foreseen outcome is quite nearby and practically the equivalent tendency as the experimental data set.

Three confirmation experiments were performed and mean is taken to find the % error. Table 7 shows confirmation trial experiments for infiltration rate. The regression analysis between experimental data (including the training data) and predicted data is shown in Figs. 15 and 16.

According to Table 8, the maximum predicted error is around 2.5% which corresponds to nearly 8 BHN and the trend of prediction data is in accordance with the

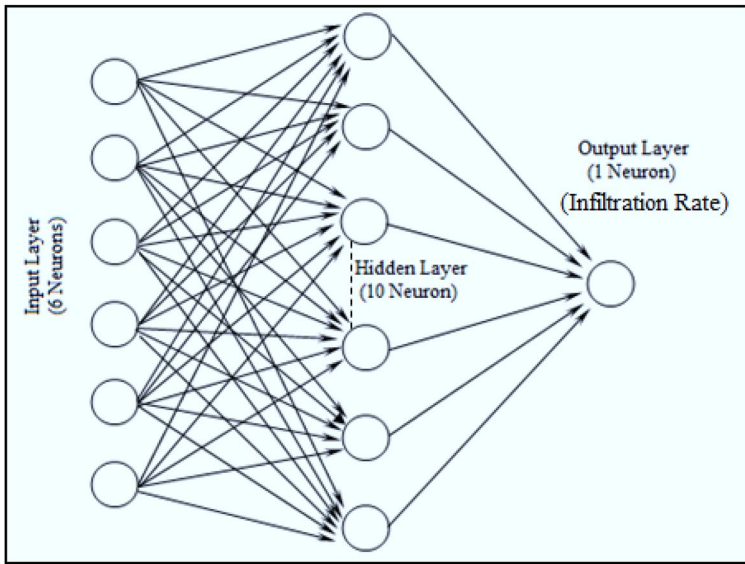


Fig. 12 Proposed Neural Structure of ANN

Table 6 MLP parameters

Parameters	Quantities
Iteration number	10,000
Input layer	6
Output layer	1
Hidden layer	10

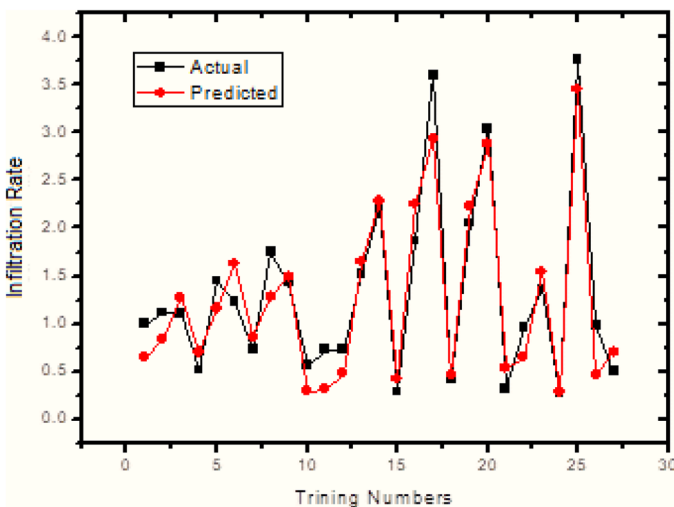


Fig. 13 Comparison in Training Output of ANN and Experimental data for Infiltration Rate

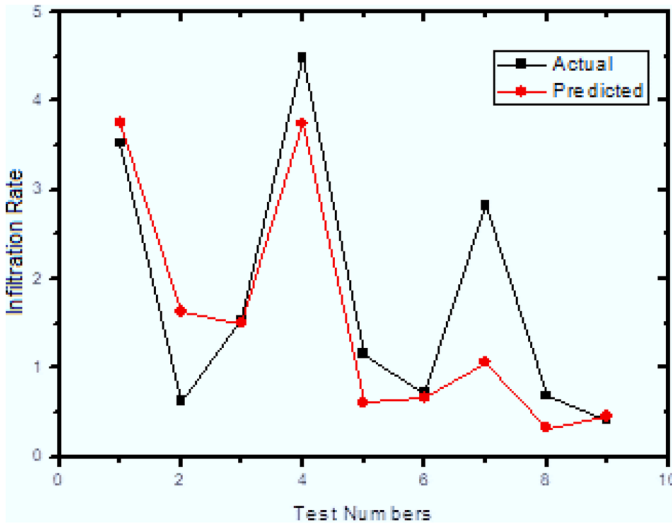


Fig. 14 Comparison in Test Run Output of ANN and Experimental data for Infiltration Rate

Table 7 Confirmation trial experiments for IR

Trial No	Inputs						Predicted IR (µm/sec.)	Actual IR (µm/sec.)
	A	B	C	D	E	F		
1	1	1	1	3	1	3	3.754	3.563
2	1	2	2	3	2	1	1.687	0.692
3	1	2	2	1	2	2	1.594	1.612
4	2	1	2	3	1	3	3.684	4.524
5	2	2	1	1	1	1	0.611	1.041
6	2	1	2	1	1	1	0.701	0.724
7	1	1	1	1	1	1	1.108	2.781
8	2	2	1	3	3	2	0.482	0.548
9	1	2	2	1	1	1	0.488	0.471

experimental values. The coefficient of correlation (R) between the output and target values explains how fit the difference in the outcome is clarified by the objectives. The value of R is one which further explains the faultless relationship between outputs and targets. In attempted work, the value for R is 0.9248 for the training data set and 0.96676 for the testing pattern, which optimum correlation. Figure 17, shows the decrement in error as the epochs are approaching its targeted value i.e., 10,000.

Fig. 15 Regression Plot for Training ANN model

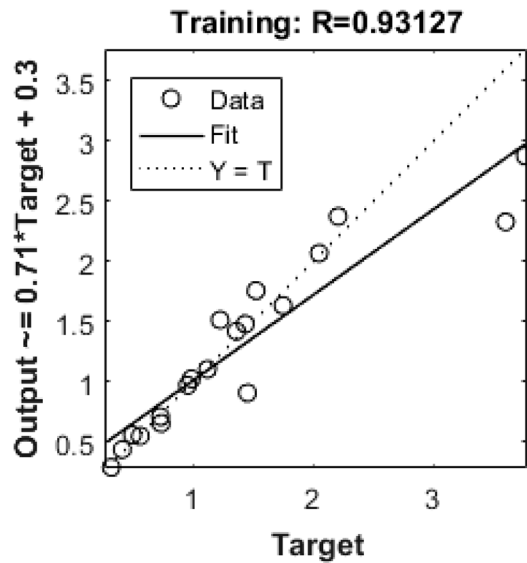
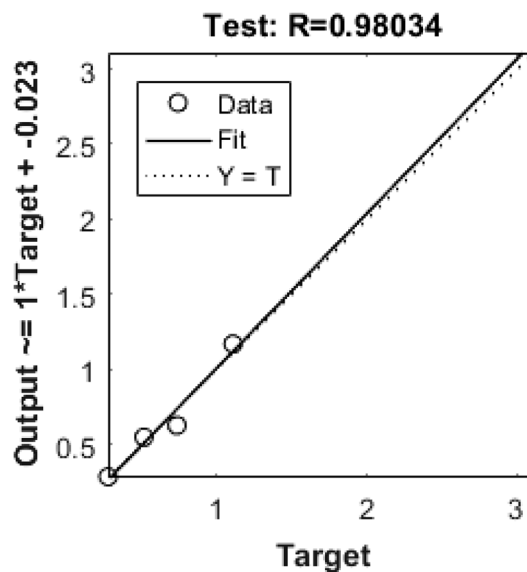


Fig. 16 Regression Plot for Testing ANN model



4 Conclusions

To examine the impact of input parameters on infiltration rate in USM of WC–Co composite material, an experimental study has been conducted. Optimization of the process parameters has also been undertaken using taguchi approach. The

Table 8 RMS Error assisted with Predictive ANN model

Test Runs	Actual	Predicted	Error	Error%	RSME
1	254.8	248.0515	6.748549	2.648567	4.771945
2	246.7	246.5582	0.141792	0.057475	0.100262
3	244.9	246.5127	-1.61267	0.6585	1.140328
4	243.2	248.243	-5.04298	2.073594	3.565926
5	246.3	247.3352	-1.03517	0.420289	0.731977
6	248.1	246.5097	1.590345	0.64101	1.124543
7	246.3	249.4141	-3.11409	1.264349	2.201995
8	253.6	247.4078	6.192187	2.441714	4.378537
9	249.9	246.1723	3.727665	1.491662	2.635857

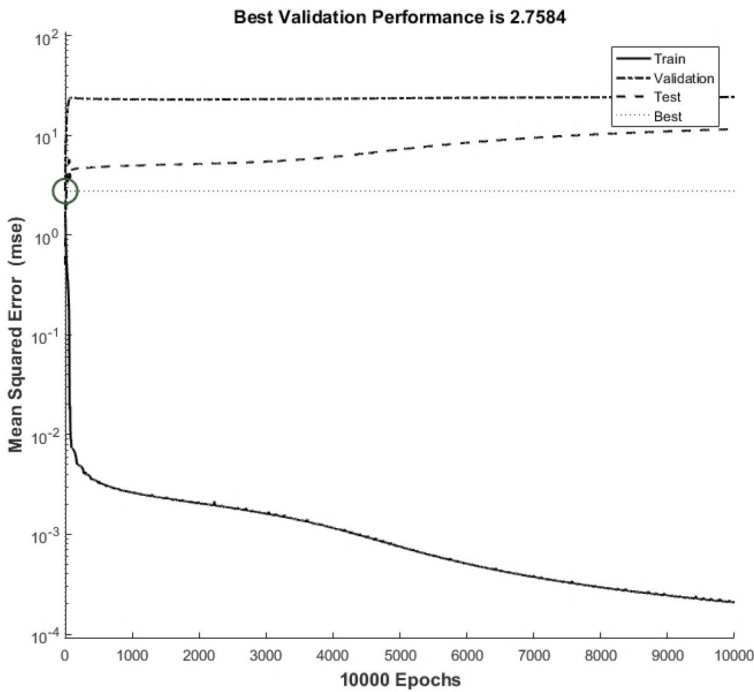


Fig. 17 Mean Squared Error Plot for Training, Validation and Test Iterations

following inferences can be drawn through this experimental and ANN modelling work based experimental study:

- Elevated infiltration proportion has been attained by employing tool as Nimonic-80A alloy. It was credited towards the fact of extensive properties (namely; hardness, and optimum impact strength) of the investigated tool sample i.e. Nimonic-80A.

- The studied factors i.e. tool materials, abrasive grit size, and power rating were attained as the majorly momentous inputs for infiltration rate. The hollow profiled tools yielded grander infiltration rate since hollow formed tools possess enhanced characteristics of abrasive flow. This finding can be contributed towards the effective flushing of the micro-formed chippings from the machining zone. The utmost infiltration rate was acquired at an amalgamation of the advanced power rating and grit size of coarse type.
- The ideal parametric combination for infiltration rate has been developed as; cobalt- 6%, work thickness- 3 mm, tool- hollow, tool material- nimonic-80A alloy, abrasive size- 200, and power rating- 80%. The presented ANN model depicts a healthy link for both training and testing facts, thereby authenticating the developed model. The higher RMS inaccuracy amid the investigational and forecasted infiltration rate was observed to be 4.7 approx.
- Microstructure analysis revealed that good edge quality with no appearance of cracks or burr/chipping on the edge of the drilled holes which further ensured the quality level of hole drilling using attempted USM process.

References

1. Singh, R. P., Singhal, S. (2018). Rotary ultrasonic machining of alumina ceramic: experimental study and optimization of machining responses. *J. Eng. Res.*, 6(1)
2. Kataria, R., Kumar, J., Pabla, B.S.: Experimental investigation and optimization of machining characteristics in ultrasonic machining of WC-Co composite using GRA method. *Mater. Manuf. Process* **31**, 685–693 (2015)
3. Cheema, M.S., Dvivedi, A., Sharma, A.K.: A hybrid approaches to multi criteria optimization based on user's preference rating. *Proc. Inst. Mech. Eng. Part B: J. Eng. Manuf.* **227**, 1733–1742 (2013)
4. Patra, K.K., Debnath, T., Patowari, P.K. (2018). Fabrication of an array of square micro-holes on glass using ultrasonic machining. In *AIP Conference Proceedings* (Vol. 1998, No. 1, p. 020013). AIP Publishing
5. Kataria, R., Singh, R.P., Kumar, J.: An experimental study on ultrasonic machining of tungsten carbide-cobalt composite materials. *AIMS Mater. Sci.* **3**(4), 1391–1409 (2016)
6. Singh, R.P., Singhal, S.: Investigation of machining characteristics in rotary ultrasonic machining of alumina ceramic. *Mater. Manuf. Processes* (2016). <https://doi.org/10.1080/10426914.2016/1176190>
7. Singh, R.P., Singhal, S.: Rotary ultrasonic machining of macor ceramic: an experimental investigation and microstructure analysis. *Mater. Manuf. Processes* (2016). <https://doi.org/10.1080/10426914.2016/1198033>
8. Singh, R.P., Singhal, S.: Experimental investigation of machining characteristics in rotary ultrasonic machining of quartz ceramic. *J. Mater. Design Appl.* (2016). <https://doi.org/10.1177/1464420716653422>
9. Wang, J., Shimada, K., Mizutani, M., Kuriyagawa, T.: Tool wear mechanism and its relation to material removal in ultrasonic machining. *Wear* **394**, 96–108 (2018)
10. Singh, R.P., Kataria, R., Singhal, S., Garg, R.K., Tyagi, M.: Hole quality measures in rotary ultrasonic drilling of Silicon Dioxide (SiO₂): investigation and modeling through designed experiments. *Silicon* **12**, 1–14 (2020)
11. Jadoun, R.S., Kumar, P., Mishra, B.K.: Taguchi's optimization of process parameters for production accuracy in ultrasonic drilling of engineering ceramics. *Prod. Eng. Res. Dev.* **3**, 243–253 (2009)
12. Singh, R.P., Kataria, R., Kumar, J., Verma, J.: Multi-response optimization of machining characteristics in ultrasonic machining of WC-Co composite through Taguchi method and grey-fuzzy logic. *AIMS Mater. Sci.* **5**(1), 75–92 (2018)

13. Kataria, R., Kumar, J.: Machining of WC-Co composites- A review. *Mater. Sci. Forum* **808**, 51–64 (2015)
14. Pradhan, S., Das, S. R., & Dhupal, D. (2020). Performance evaluation of recently developed new process HAJM during machining hardstone quartz using hot silicon carbide abrasives: an experimental investigation and sustainability assessment. *Silicon*, 1–25
15. Ross, P.J.: *Taguchi Techniques for Quality Engineering*. McGraw Hill, New York (1996)
16. Jha, K., Kumar, R., Verma, J., Kataria, R.: Nonlinear modelling of roughness parameters in finish turning of EN31 high carbon steel. *Int. J. Mach. Mach. Mater.* **20**(5), 460–473 (2018)
17. Tan, P.N.: *Introduction to Data Mining*. Pearson Education, India (2007)
18. Mathieu, J.E., Tannenbaum, S.I., Salas, E.: Influences of individual and situational characteristics on measures of training effectiveness. *Acad. Manag. J.* **35**(4), 828–847 (1992)
19. Singh, R., Singh, R.P., Trehan, R. (2020). State of the art in processing of shape memory alloys with electrical discharge machining: a review. *Proceedings of the Institution of Mechanical Engineers, Part B: Journal of Engineering Manufacture*, 0954405420958771

Publisher's Note Springer Nature remains neutral with regard to jurisdictional claims in published maps and institutional affiliations.